ISSN1027-5495. Functional Materials, 32, No.3 (2025), p. 487-497
doi:http://dx.doi.org/10.15407/fm32.03.487 © 2025 — STC "Institute for Single Crystals"

Quaternary crystals CdZnTeSe: Growth via the vertical Bridgman method with different compositions of raw materials

S.V. Naydenov[1], O.K. Kapustnyk[1], I.M. Pritula[1], D.S. Sofronov[1], I.S. Terzin[1], N.O. Kovalenko[1,2]

[1] Institute for Single Crystals, SSI "Institute for Single Crystals", National Academy of Sciences of Ukraine, 60 Nauky Ave., 61072 Kharkiv, Ukraine
[2] Helmut-Schmidt-Universität, Holstenhofweg 85, 22043 Hamburg, Germany

Received August 8, 2025

Indium-doped semiconductor crystals CdZnTeSe with various compositions were grown via the vertical Bridgman method under high-pressure argon. For the first time, these crystals were obtained via a combined method from a mixture of single and binary starting components. A theoretical analysis of the permissible reactions for obtaining multicomponent CdZnTeSe crystals from various compositions of starting materials was performed. The homogeneity of the distribution of the atomic composition of the obtained crystals and the electrical resistance (in the dark and under illumination) were studied. Crystals grown via the new combined method demonstrated the best homogeneity of composition and electrophysical properties.

Keywords: Crystal growth, High Pressure Bridgman method, Semiconductors II-VI, CdZnTeSe solid solutions, In-doped materials

Кватернарні кристали CdZnTeSe:In вирощені вертикальним методом Бріджмена із різних композицій ростових речовин. *С.В. Найденов, О.К. Капустник, І.М. Притула, Д.С. Софронов, І.С. Терзін, Н.О. Коваленко*

З декількох різних композицій стартових матеріалів вирощені леговані індієм напівпровідникові кристали CdZnTeSe:In за допомогою вертикального методу Бріджмена під високим тиском аргону. Вперше отримані кристали комбінованим способом із суміші простих та бінарних компонентів. Виконано теоретичний аналіз допустимих способів отримання багатокомпонентних кристалів CdZnTeSe із різних композицій ростових складових. Проведено дослідження однорідності розподілу атомних складових та електричного опору (в темряві та при освітленні) зазначених кристалів. Виявлено, що найбільша однорідність складу та електрофізичних властивостей властива кристалам, що були вирощені новим комбінованим способом.

1. Introduction

CdTe-based semiconductor crystals are widely used as infrared and radiation detectors. The ternary crystal CdZnTe (CZT) is well known and has been used for X-ray and gamma-ray detection at room temperature [1]. However, among semiconductor crystals it is difficult to grow [2]. Various drawbacks [3] and the relatively low yield of detector material during CZT growth are associated with the "poor" thermophysical properties of the melt-crystal system, as well as the "soft-brittle" structure of the CdTe parent matrix. During the growth of these crystals, there is a strong tendency for the formation of intrinsic and impurity especially at elevated growth temperatures and/or melt contamination. They have low activation energies of

extended (growth) defects, a large degree of ionic chemical bonding, high variability of the Fermi level in the band gap with changing impurity composition, and non-stoichiometry of the composition due to strong segregation and/or increased volatility of some atomic components.

Long-term efforts to improve CZT crystal fabrication technology have not led to the expected results, although these crystals continue to be widely grown, mainly from solution melts, via the THM method. Recently, new quaternary CdZnTeSe (CZTS) crystals have been proposed as alternatives [4]. Theory [5] and experiments [6, 7] indicate that there is a "hardening" effect due to the addition of a small amount of selenium. When selenium is added, the excess Gibbs energy of solid solution formation is thermodynamically reduced, making the destruction of the crystalline structure energetically less favorable. As a result, the number of the most harmful defects (clusters of small grains, dislocation networks, large tellurium inclusions, etc.) in CZTS crystals can be reduced.

Although CZTS crystal growth methods are mainly (apart from some technological nuances) the same as CZT crystal growth methods are, there are some differences. In melt methods such as High-Pressure Bridgman Method (HPBM) [8-11] or Vertical Freezing Gradient (VFG) method [12], ternary CZT crystals are usually synthesized and/or grown from a mixture of three simple components: cadmium, tellurium and zinc. In this case, the large zinc segregation coefficient of 1.24-1.35 (see, for example, [2]) leads to significant inhomogeneity in the ingot composition. Synthesis of CZT by adding (in batch) zinc to the binary compound CdTe gives inferior results. In the Travelling Heater Method (THM) [13, 14], CZT is grown by zone melting from solution-melt containing dissolved cadmium and zinc with excess tellurium (more than 50% of the total solution volume). In this case, it is preferable to use either simple substances or a batch of pre-synthesized CZT polycrystals as growth raw materials. CZTS quaternary crystals contain four atomic elements: cadmium and zinc, tellurium and selenium. This increases the permissible set of raw material combinations. Potentially, such crystals can be grown from significantly different compositions of starting materials (see below for more details). Ternary CZT crystals can be grown from both non-compound source materials (a mixture of cadmium, zinc and tellurium) and compound source materials (e.g., a mixture of cadmium telluride with zinc or the CZT substance itself). In the first case, the melting temperature of the individual components of the raw material is different; in the second case, it can be the same if a single crystal is grown from a polycrystalline material. CZTS crystals are more often grown from a complex composition of several starting components. The melting temperatures and mutual solubilities of these materials in the melt can vary greatly. This feature initially makes it difficult to obtain a homogeneous crystalline material. However, it is from homogeneous crystals that the highest quality detector elements are made.

The specificity of the growth of multicomponent semiconductor A2B6 crystals is that they are highly sensitive to changes in growth conditions, including the choice of loading of initial growth components. Typically, CZTS crystals are grown from starting material in the form of a composition of "CZT+CdSe" ternary CZT with a selenium precursor [15] or a composition of four simple components, "Cd+Zn+Te+Se", e.g., [16], or a composition of binary components, "CdTe+ZnTe+CdSe", e.g., [17]. The question naturally arises as to which method of selecting the starting material gives the best results for obtaining the most homogeneous crystalline ingots with a high yield of useful material and acceptable properties. Previously, this problem was considered for CZT ternary crystals [18]. In this work, quaternary CZTS crystals with different compositions of growth components were grown via the vertical Bridgman method under high argon pressure. A comparison of their homogeneity and electrophysical properties was carried out depending on the change in composition. This made it possible to identify two promising methods for growing CZTS crystals from a melt: (1) with a starting material consisting only of binary components CdTe, ZnTe and CdSe and (2) a *new combined method* of growing from two simple components Cd and Te and two binary components ZnTe and CdSe. Note, that to our knowledge, the combined method has not been proposed previously.

2. Theoretical analysis

CZTS solid solution as a chemical compound can be obtained through various reactions. For example, a reaction of synthesis of a solid solution from its constituent binary components can be used

$$(1-x-y)\mathrm{CdTe}+x\mathrm{ZnTe}+y\mathrm{CdSe}\rightarrow \rightarrow \mathrm{Cd_{1-x}Zn_xTe_{1-y}Se_y}, \quad (1)$$

or synthesis from simple components alone

$$(1-x)\mathrm{Cd}+x\mathrm{Zn}+(1-y)\mathrm{Te}+y\mathrm{Se}\rightarrow \rightarrow \mathrm{Cd_{1-x}Zn_xTe_{1-y}Se_y}, \quad (2)$$

or synthesis of a ready-made CZT ternary compound with a selenium precursor in the form of CdSe

$$(1-y)\mathrm{Cd_{1-x}Zn_xTe}+y\mathrm{CdSe}\rightarrow \rightarrow \mathrm{Cd_{1-x+xy}Zn_{x-xy}Te_{1-y}Se_y}. \quad (3)$$

In the latter case, $\mathrm{Cd_{1-x+xy}Zn_{x-xy}Te_{1-y}Se_y}\approx\mathrm{Cd_{1-x}Zn_xTe_{1-y}Se_y}$ provided that the atomic concentrations x<<1 and y <<1 of the solid solution are small, when their product can be neglected as a value of a higher order of smallness, xy<<{x,y}<<1. Other reactions are also possible.

The most general type of reaction for the synthesis of CZTS from binary components is as follows:

$$(1-x-y-z)\mathrm{CdTe}+x\mathrm{ZnTe}+y\mathrm{CdSe}+z\mathrm{ZnSe}\rightarrow \rightarrow \mathrm{Cd_{1-x-z}Zn_{x+z}Te_{1-y-z}Se_{y+z}}. \quad (4)$$

The synthesis of a material from several simple and binary components is possible. For example, one can formally use such a reaction

$$(1-x-y)\mathrm{Cd}+(1-x-y)\mathrm{Te}+x\mathrm{ZnTe}+y\mathrm{CdSe}\rightarrow \rightarrow \mathrm{Cd_{1-x}Zn_xTe_{1-y}Se_y}. \quad (5)$$

Even more exotic is the reaction that is obtained by combining the reactions (1) and (5). The reagents supplying cadmium and tellurium atoms to the system include both the simple components themselves and their binary component CdTe:

$$(1-x-y-z)\mathrm{CdTe}+x\mathrm{ZnTe}+y\mathrm{CdSe}+ +z\mathrm{Cd}+z\mathrm{Te}\rightarrow \mathrm{Cd_{1-x}Zn_xTe_{1-y}Se_y}. \quad (6)$$

Note that here the concentration z of additional simple components remains arbitrary. The full list of permissible reactions is rather wide and is not given here. Despite this diversity, practical conditions for CZTS crystal growth impose certain restrictions on the choice of initial reagents.

In the general reaction (4) , the binary compound ZnSe could be used to introduce zinc and selenium into CZTS. However, ZnSe has a high melting point (1525°C), which far exceeds the melting point of the other growth components and the melting point of CZTS (1150-1180°C) at which crystals grow from the melt. In addition, almost all the chalcogenides under consideration are very poorly soluble even at high temperatures. In addition to purely molecular reasons, this is due to the high viscosity of melts based on cadmium selenide. Moreover, high-melting chalcogenides dissolve significantly worse than other chalcogenides. For these reasons, the growth of monophase CZTS crystals by the melt method becomes impossible if the binary component ZnSe is present in the composition of the raw material even in insignificant amounts (a few atomic or mass percentages). We confirmed this by attempting to grow such CZTS crystals using the Bridgman method.

It is possible to incorporate selenium into CZTS crystals directly via reaction (2). However, the simple components zinc and selenium are present in the raw material. At high melt temperatures, the exothermic reaction of zinc selenide formation can start. It is accompanied by the release of large amounts of heat and is explosive in nature. Therefore, for a more controlled introduction of selenium into the CZTS, we chose the method of adding the binary component CdSe. The disadvantage of this method is the excessive contamination of cadmium selenide [19], for which, even with modern purification methods, the required purity of 99.9999% (6N), which is inherent to all other growth components, has not yet been achieved.

The growth of CZTS crystals from the CZT compound via the Bridgman method (3) has not been shown to produce crystalline ingots with a uniform distribution of selenium. The selenium concentration can vary several times along the length of the ingot (see Section 4). In our opinion, this is also due to the poor mutual solubility of chalcogenides in the melt. Moreover, this negative effect increases with the transition from binary to ternary compounds, i.e., from the CdTe melt to the CZT melt.

Finally, CZTS can be grown (synthesized) via a complex reaction of type (5) , in which both simple and binary components participate simultaneously. Strictly speaking, in this method, CdTe is first synthesized from the melt of cadmium and tellurium (elementary bimolecular chemical reaction), and only then, at sufficiently high temperatures and after complete dissolution of all binary components ZnTe and CdSe in the CdTe melt, CZTS crystals are grown. The advantage here is that the binary

components are much better dissolved in cadmium, and tellurium melts at intermediate synthesis stages. This generally leads to better mutual dissolution of all the components and homogenization of the final melt.

It is useful to compare the thermodynamic equilibrium constants for the reactions (1) and (5). For simplicity, let us consider the CZTS melt as an ideal solution. Then, for saturated vapors above the melt, Raoul's law [20] is satisfied, and their pressure is proportional to the concentration of components in the melt. This allows us to write the equilibrium constant for the reaction of CZTS synthesis from the composition of binary components in the form

$$K_{binary}(T,p) = \left[\frac{p_{CZTS}}{p^0_{CZTS}}\right]\left\{\left[\frac{p_{CdTe}}{p^0_{CdTe}}\right]\left[\frac{p_{ZnTe}}{p^0_{ZnTe}}\right]\left[\frac{p_{CdSe}}{p^0_{CdSe}}\right]\right\}^{-1}, \quad (7)$$

and for the combined synthesis in the form

$$K_{comb}(T,p) = \left[\frac{p_{CZTS}}{p^0_{CZTS}}\right]\left\{\left[\frac{p_{Cd}}{p^0_{Cd}}\right]\left[\frac{p_{Te_2}}{p^0_{Te_2}}\right]^{1/2}\left[\frac{p_{ZnTe}}{p^0_{ZnTe}}\right]\left[\frac{p_{CdSe}}{p^0_{CdSe}}\right]\right\}^{-1}, \quad (8)$$

where T is the temperature, p is the external pressure, $[p]$ is the saturated vapor pressure of partial components above the melt, and the upper index "0" denotes bringing the system to standard conditions. When obtaining the formula, the fact was taken into account that atomic tellurium, when evaporated from the melt, turns into a molecular diatomic gas. Combining these expressions, we obtain the relation

$$K_{binary}(T,p) \approx \approx K_{comb}(T,p)\left[\frac{p_{Cd}}{p^0_{Cd}}\right]\left[\frac{p_{Te_2}}{p^0_{Te_2}}\right]^{1/2}\left[\frac{p_{CdTe}}{p^0_{CdTe}}\right]^{-1}. \quad (9)$$

At the CZTS melting temperature, the vapor pressure of cadmium above the melt reaches several tens of atmospheres (the most volatile component), the vapor pressure of tellurium reaches several atmospheres, and the vapor pressure of cadmium telluride does not exceed the atmospheric pressure (approximately 10^5 Pa). Therefore, the condition is satisfied with good accuracy:

$$K_{comb}(T,p) \sim \sim 10^{-2} K_{binary}(T,p) \ll K_{binary}(T,p). \quad (10)$$

In the case of a weakly concentrated CZTS solid solution, $x \ll 1, y \ll 1$, the Gibbs energies for the reactions under consideration can be related to the simple expression

$$\Delta G_{comb} \approx \Delta G_{binary} + RT \ln\left(\frac{Q_{comb}}{Q_{binary}}\right), \quad (11)$$

where ΔG is the difference in the chemical potentials of the products and reactants taking into account stoichiometry coefficients (it is assumed that the reaction proceeds, $\Delta G \le 0$); Q is the quotient of the corresponding reactions; R is the gas constant. When approaching a state of thermodynamic (chemical) equilibrium, the factor Q tends to the equilibrium constant. For simplicity, let us assume that $Q \approx K(T,p)$. Then, the formulas (10) and (11) follow the relation

$$|\Delta G_{comb}| = |\Delta G_{binary}| + \alpha RT, \quad (12)$$

where $\alpha \sim 1$ is of the order of unity. The difference in the Gibbs energies of solid solution formation for these reactions can reach values of several RT, which are quite large at characteristic CZTS melt temperatures. The ratio indicates that when the parameters of the system change (approaching equilibrium), the Gibbs energy of the combined reaction decreases significantly more than in the case where the reaction is carried out on the basis of binary components. At the physical level, this corresponds to faster synthesis and uniform homogenization of the CZTS melt, all other growth conditions being equal. As a result, the ability to obtain more homogeneous CZTS crystals is promoted.

Considering the results of the theoretical analysis, among all possible methods of CZTS crystal production from melt, two most promising options should be highlighted: *synthesis from binary components* according to reaction (1) and joint synthesis according to reaction (5). The experimental growth of the CZTS crystals confirmed this conclusion. Both the synthesis and the final growth of CZTS crystals from the melt are carried out in the same growth process to avoid contamination during reloading of synthesized material and to reduce material and time costs.

3. Experimental part

CZTS crystals with diameters of up to Ø25 mm (1 inch) and lengths of up to 60 mm were grown via the vertical Bridgman method under high-pressure argon (6N). Crystals were grown in a single-zone furnace with automatic

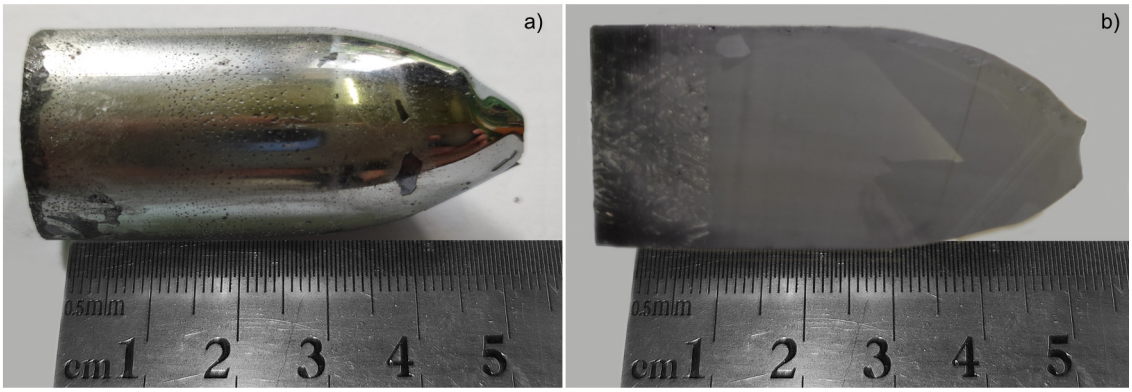

Fig. 1. CZTS-2 crystal ingot (a) and cut plate (b) with the starting composition "CZT:In + CdSe".

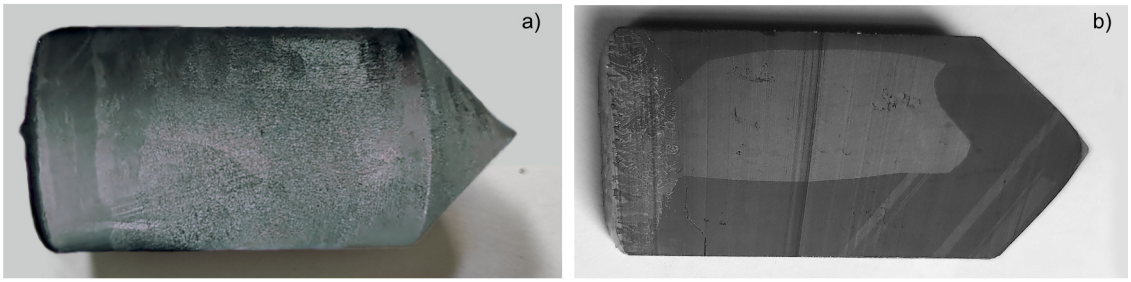

Fig. 2. CZTS-5 crystal ingot (a) and cut plate (b) with the starting composition "CdTe+ZnTe+CdSe+In".

control of the temperature and crucible speed. The temperature in the melt was monitored by a W-Re thermocouple. The starting materials used for growth were 99.9999% pure (6N), except for a CdSe batch with a purity of 99.9995% (5N5). The raw materials were not crushed before loading. For different compositions of the starting materials, the phase composition was calculated using the stoichiometric formula of the solid solution $Cd_{0.9}Zn_{0.1}Te_{0.98}Se_{0.02}$ and corresponded to the same concentration of zinc and selenium in the load for all the growths.

The starting material was loaded under high-purity conditions into a precleaned graphite crucible made of dense low-ash graphite with a purity of 5N-6N. In a number of cases, including when growing CZTS from presynthesized CZT, a quartz ampoule with an internal diameter of ∅25 mm was used as a crucible. The optimal growth regime was selected based on the choice of starting material and the use of different synthesis reactions. The melt temperature in all cases was slightly higher than the melting point of CZTS, and the temperature gradient at the crystallization front was chosen to be 20°C/cm. Prior to the crystal growth stage, the melt was incubated for 24 h to ensure maximum homogenization. The argon pressure in the active phase of growth reached 22–24 atm. No seed crystals were used. Spontaneous nucleation starts from the conical part of the crucible (spout) and then continues on its sidewalls. The crystal growth rate did not exceed 0.8 mm/hour. With the optimal choice of the mode, a large-block crystalline ingot with fine twinning in single-crystal grains was obtained at the output. Growth losses due to material entrainment usually do not exceed 3–6%. When growing crystals in quartz ampoules, material entrainment was significantly greater than when growing in graphite crucibles. To compensate for doping, an indium donor impurity was used with a target concentration in the crystal of about 10 ppm on average. This allows us to obtain high-resistivity indium-doped CZTS:In crystals.

The used growth mode was the same for all crystals and mainly did not depend on the choice of starting materials. Figures 1-4 show photographs of the obtained CZTS:In crystal ingots. 5 mm thick longitudinal plates were cut from the central part of the ingots. After cleaning the plate from contaminants, the crystalline quality of the material was visually assessed, including the composition of single-crystal bars, the presence of twins, clusters of small grains, growth inclusions and chips, and other visually visible defects. X-ray powder diffractometry of

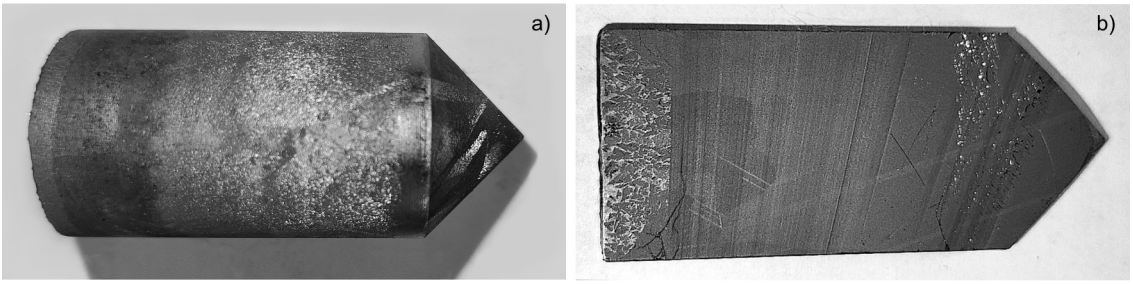

Fig.3. CZTS-7 crystal ingot (a) and cut plate (b) with the starting composition "CdTe+ZnTe+CdSe+Cd+Te +In".

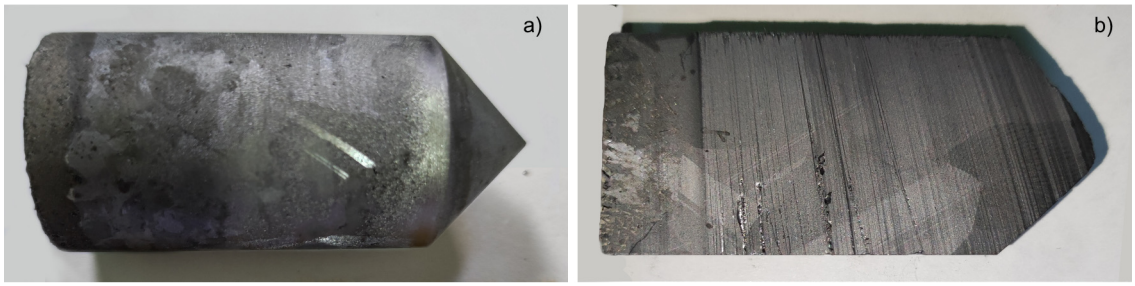

Fig. 4. CZTS-8 crystal ingot (a) and cut plate (b) with the starting composition "Cd+Te+ZnTe+CdSe+In".

the obtained solid solution crystals confirmed their monophase composition. X-ray studies of the crystal structure of the obtained crystals (rocking curves, etc.) will be carried out in further studies.

Mapping of the atomic composition and electrical resistivity in the dark and under illumination was performed for mechanically processed plates (chemical polishing was not applied). The spatial step of the measurements along the ingot axis was 4–5 mm. The atomic composition variations were determined by X-ray electron density spectroscopy on a low-vacuum scanning electron microscope (JSM-6390LV) with an AZtech Energy X-max 50 detector analyzer. The accuracy of the composition measurements is estimated to be approximately 0.5 at.%. When the composition was mapped, areas containing tellurium phases or other micro-inclusions that are not characteristic of the matrix itself were excluded from the observation field.

The variations in the electrophysical parameters were investigated using a noncontact expression method (without applying ohmic contacts to the surface of the samples) on a special stand with an E6-13A tera-ohmmeter (USSR) at a constant applied voltage of 100 V. The direct current was applied step by step from opposite sides of the plate at points opposite each other. To protect against possible surface leakage currents, special current collectors with silicone pressure rings are used on the contacts. The stand was recalibrated on test samples of high-resistance semiconductor crystals with known resistance. The measurements were repeated several times at each step to improve the statistics. The errors in measuring the resistance of high-resistivity samples (10^{11}-10^{12} Ohm) are estimated to be in the order of giga-Ohm. The conductivity type was controlled by measuring the thermal EMF (the Seebeck effect). All the samples were found to have *p*-type conductivity.

4. Results and discussion

The results of atomic composition mapping of CZTS crystals (see Figs. 1-4) obtained from different starting materials are presented in Fig. 5. The diagrams show the zinc and selenium contents in atomic percentages. The distances along the abscissa axis correspond to the measurement points at the transition along the ingot axis from the tip to the heel. Variations in the cadmium and tellurium components along the ingot were obtained but are not given here. The relative values are not as significant as the variations in zinc and selenium content, except for a 10–15 mm long transition region at the end of the ingot. The boundary of this region is clearly visible in Figs. 1-4. In this growth zone,

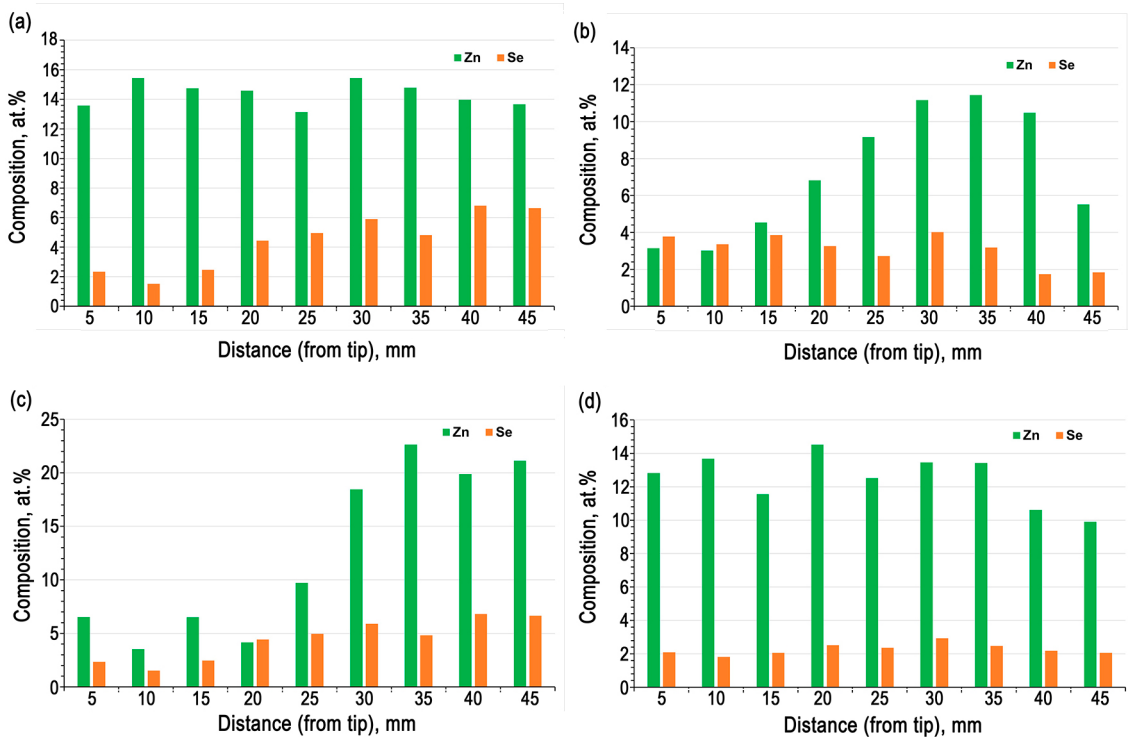

Fig. 5. Spatial distributions of Zn (at.%) and Se (at.%) across the grown crystal ingots: CZTS-2 (a); CZTS-5 (b); CZTS-7 (c); CZTS-8 (d).

the melt solidification occurs too quickly, the stoichiometry is greatly disturbed (a large excess of tellurium is accumulated), and crystals do not form. As the measurements show, the total molar concentrations of "Cd+Zn" cations and "Te+Se" anions are always close to unity. Deviations in the cation-anion balance usually do not exceed 1 at.% which is explained by the overall accuracy of measurements – errors in determining the composition of cations and anions of 0.5 at.%.

As shown in Fig. 5, for the CZTS-2 crystal grown from the initial composition "CZT+CdSe" and the CZTS-7 crystal grown from the composition "CdTe+ZnTe+CdSe+Cd+Te", the distribution of selenium is not homogeneous enough. For the CZTS-5 crystal grown from the composition "CdTe+ZnTe+CdSe+CdSe", the selenium distribution is more homogeneous. The CZTS-8 crystal grown from the "Cd+Te+ZnTe+CdSe" composition is almost ideal.

The distributions of zinc in the CZTS-5 and CZTS-7 crystals are highly inhomogeneous. This is due not only to the significant segregation of zinc at the crystallization front but also, perhaps to an even greater extent, to the poor solubility of binary components in the cadmium telluride melt. Increasing the melt homogenization time to overcome these harmful effects is not advisable, as it leads to strong evaporation of volatile components (cadmium and zinc) and a violation of stoichiometry. The distribution of zinc in the CZTS-2 crystal is more homogeneous. This is due to the growth of the CZTS crystals from the selected pre-synthesized polycrystalline CZT, in which the zinc distribution was initially quite homogeneous. It should be noted that CZTS-8 crystals obtained by the combined method without pre-synthesis have high homogeneity in the distribution of the zinc component. A slight decrease in the zinc content here occurs only at the end of the crystal and is due to the segregation effect.

In comparison with the results of other works on growth of homogeneous CZTS crystals using the Bridgman method, we have obtained more homogeneous crystals. In our crystals, the relative variation of zinc content (the element with the highest segregation coefficient) across the ingot is within is within 5-15% of the nominal value, whereas when grown using other methods, this variation often exceeds 20-30% (see, for example, [23]), and sometimes can even approach 50-60% (see, for example, [24]).

Thus, a comparison of the compositions of the obtained crystals indicates that the CZTS crystals obtained by the combined method from the starting material "CdTe+ZnTe+CdSe+Cd+Te"

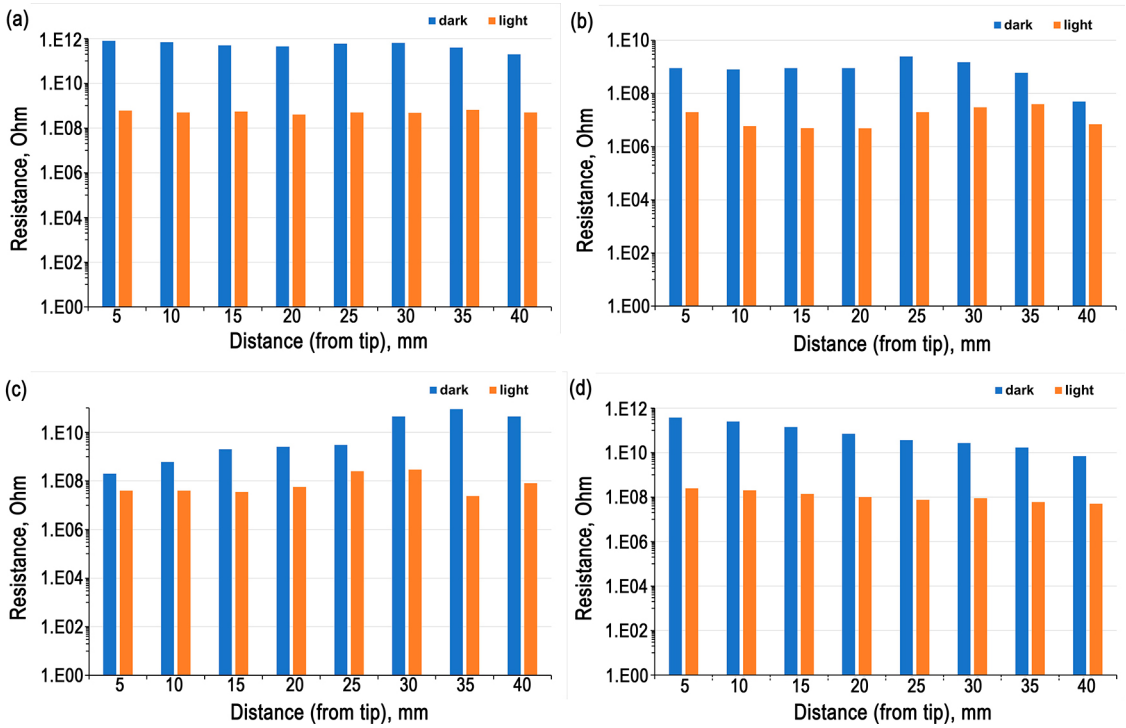

Fig. 6. Spatial distributions of electric resistance (Ohm) in the dark and photoresistance under illumination across the grown crystal ingots: CZTS-2 (a); CZTS-5 (b); CZTS-7 (c); CZTS-8 (d).

have the highest homogeneity in Zn and Se components. The physical reasons for this homogeneity were explained on the basis of thermodynamic considerations at the end of Section 2. These results are associated with a higher rate of decrease in the Gibbs energy during the formation of a solid solution from the specified composition of reagents (starting raw materials).

Measurements of the composition of the grown CZTS:In crystals were complemented by measurements of their electrical resistance in the dark and in the light under illumination by a 100 W halogen lamp. These data are shown in Fig. 6. Resistance mapping of plates cut from crystals was carried out at the same points as the atomic composition measurements. The concentration of the indium dopant (when loading the raw material) for these crystals differed several times. Considering the very low distribution coefficient of In (no more than 0.1), its concentration in the charged state was approximately an order of magnitude greater (from 30 to 100 ppm) than in the crystalline state.

The variation in the electrical resistivity of a material depends on many factors. The variation in the dark resistance mainly depends on the position of the Fermi level in the band gap. If full compensation has not occurred during doping of the crystal, i.e., the Fermi level is still far from the middle of the band gap, then the change in composition does not greatly affect the resistance variation. These CZTS samples have low resistivity (typically 10^6–10^8 Ohm·cm or lower), that is virtually indistinguishable from the illuminated resistivity. If the compensation is strong enough, the dark resistance is sensitive to variations in the crystal composition, especially to variations in the zinc content of the crystal, since the band gap width changes [21]. However, the most significant changes in dark resistance are associated with changes in the concentration of the compensating dopant.

Segregation of the dopant at the crystallization front leads to its inhomogeneous distribution in the crystal. With good melt mixing, the dopant distribution in the crystal is described by the Sheil formula [22]:

$$C(x) = kC_0(1-x)^{k-1}, \qquad (13)$$

where C is the concentration of dopant in the crystal; C_0 is the initial concentration of dopant in the charge; k is the distribution (segregation) coefficient; and x is the fraction of volume that has crystallized. In this case, the parameter x corresponds with good accuracy to the longitudinal coordinate along the crystal

growth axis, i.e., at the points of measurements of the composition and resistivity. Considering the smallness of the indium distribution coefficient $k \ll 1$, the expression (13) can be simplified as follows:

$$C(x) \approx kC_0(1+\alpha x), \qquad (14)$$

where α is a correction factor associated with deviations of the actual distribution of the dopant from the model formula (13), including those due to inhomogeneous initial loading of the dopant and poor melt mixing. Usually, to avoid strong heterogeneity (across the crystal), indium in the batch is placed entirely in the lower part of the crucible, from which crystal growth begins. During crystal growth, excess indium, which constantly appears at the crystallization front, easily diffuses into the region of the melt that is initially depleted in indium. As a result, there is an effective equalization of the indium concentration and partial compensation of the segregation effect. The indium content in the obtained crystal often decreases from the beginning to the end of the ingot. In contrast, with a uniform initial distribution of indium, the indium concentration should increase from the beginning to the end of the ingot.

The resistivity of a semiconductor depends exponentially on the position of the Fermi level relative to the edges of the band gap. In a compensated (high resistivity) semiconductor, the Fermi level is near the middle of the band gap. With a small change in the concentration of the compensating dopant, the Fermi level shifts in the band gap proportionally to this concentration. As a result, the resistivity changes in accordance with the local change in the concentration of the dopant. Moreover in this case, the logarithm of the dark resistivity should change in a linear way, similar to the change in the concentration of the dopant in the crystal:

$$\ln\rho(x) \approx (1+\beta x)\ln\rho_0, \qquad (15)$$

where β and ρ_0 are constant values for this crystal.

Fig. 7 shows the distributions of the logarithm of resistance for the CZTS crystals. Since the test samples were fabricated as identical plates, their resistivity (when measured at different points) is proportional to the normal resistivity with good accuracy (we neglect leakage currents). The dark resistivity of the CZTS-2 sample does not much along the ingot. This is due to the increased (100 ppm in the feedstock for CZT synthesis) and homogeneous

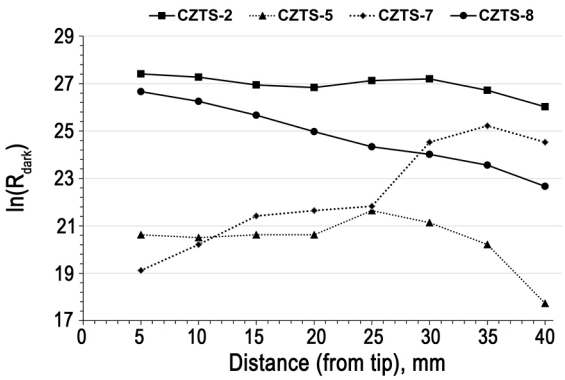

Fig. 7. Spatial dependence of the logarithm of the dark resistance (Ohm) for different crystal ingots.

indium content in the starting material from which CZTS-2 was grown. Here, there is a strong compensation of the position of the Fermi level in the band gap. The resistivity of the ingot becomes maximal, and its variations are hardly noticeable. This corresponds to the case where $\alpha \ll 1$ in the formula (14). In contrast to the CZTS-2 sample, the CZTS-5, CZTS-7, and CZTS-8 crystals had the same moderate loading of 40 ppm indium during growth. The material compensation was incomplete. As a result, the CZTS-5 and CZTS-7 crystals exhibit strong heterogeneity in the distribution of resistivity ($\ln\rho$) across the ingot, which does not agree well with the expected relationship. Particularly strong variations are characteristic of the CZTS-7 crystal. This is due to poor melt homogenization, which leads to significant inhomogeneities in both the basic composition and the indium dopant in the crystal ingot. At the same time, the CZTS-8 crystal shows an almost linear dependence corresponding to formula (14). Consequently, it is the most "homogeneous" in terms of changes in electrophysical properties. Strictly speaking, in terms of electrical resistivity, the CZTS-8 crystal has high local homogeneity (in some parts of the ingot) but low global homogeneity (throughout the ingot). Its global heterogeneity is due to strong indium segregation resulting from underloading, so Fermi level compensation is incomplete throughout the crystal. By increasing the indium concentration in the loading mixture to 60-100 ppm, this harmful effect can be reduced.

In contrast to dark resistance, the photoresistance of crystals under sufficiently powerful irradiation depends to a greater extent not on the concentration of fully ionized impurities but on the concentration of generated intrinsic charge carriers (electrons and holes).

Their concentration at the same illumination intensity depends on the width of the band gap. Therefore, the most homogeneous crystals in composition (with a practically unchanged band gap) have the smallest variations in photoresistance. A close comparison of the data in Fig. 6 shows that the average relative changes in resistance of the CZTS-5, CZTS-7, and CZTS-8 crystals are 74%, 82%, and 34%, respectively. Thus, the CZTS-8 crystal has the best resistance homogeneity both in the dark and in the light.

Based on the obtained results, it can be concluded that the crystal grown by the combined method from the starting material "Cd+Te+ZnTe+CdSe" has the best homogeneity of electrophysical parameters.

5. Conclusions

Quaternary CZTS:In crystals grown from a melt with different compositions of the initial raw material were studied. It was shown that when grown from a combined initial material "Cd+Te+ZnTe+CdSe", crystals with the best composition homogeneity (almost uniform distribution of zinc and selenium components in the crystalline ingot) and high homogeneity of electrophysical properties (proportionality between the logarithm of the dark resistance of the material and the concentration of the compensating indium dopant, as well as small variations in photoresistance in different areas of the crystalline ingot) are obtained. This is due to better dissolution of binary components in the mixed melt of cadmium and tellurium, as well as better homogenization of the resulting CZTS melt under identical growth conditions. The physical mechanism of these effects is due to the higher rate of decrease in the Gibbs energy of solid solution formation as the system tends to a state of thermodynamic equilibrium compared to other reactions permitted for the synthesis of multicomponent crystals. Quaternary CZTS crystals with satisfactory homogeneity are also obtained by growing from the starting composition of binary components "CdTe+ZnTe+CdSe". However, to eliminate significant compositional variations inherent in such crystals, it is necessary to use special growth techniques, which discussed separately.

Acknowledgements

We would like to express our sincere gratitude to Dr. Pavel V. Mateichenko for performing the EDS-measurements by the scanning electron microscope.

References

1. Md.D. Alam, S.S. Nasim, S. Hasan, Recent progress in CdZnTe based room temperature detectors for nuclear radiation monitoring, *Progress in Nuclear Energy* **140**, 103918 (2021). https://doi.org/10.1016/j.pnucene.2021.103918
2. E. Dieguez, Chapter 3.04 - Growth of Cd0.9Zn0.1Te Bulk Crystals, in: *Comprehensive Semiconductor Science and Technology*, vol. **3**, Elsevier B.V., 2011, pp. 170-201. https://doi.org/10.1016/B978-0-44-453153-7.00091-2
3. Z. Li, J. Cheng, F. Liu, Q. Wang, W.-W. Wen, G. Huang, Z. Wu, Research on the technological progress of CZT array detectors, *Sensors* **24**(3), 725 (2024). https://doi.org/10.3390/s24030725
4. U.N. Roy, G.S. Camarda, Y. Cui, R. Gul, Ge Yang, J. Zazvorka, V. Dedic, J. Franc, R.B. James, Evaluation of CdZnTeSe as a high-quality gamma-ray spectroscopic material with better compositional homogeneity and reduced defects, *Scientific Reports* **9**, 7303 (2019). https://doi.org/10.1038/s41598-019-43778-3
5. S.V. Naydenov, I.M. Pritula, Hardening of multicomponent CdZnTeSe solid solutions: a theoretical approach, *Appl. Phys. A* **129**, 812 (2023). https://doi.org/10.1007/s00339-023-07109-8
6. U.N. Roy, G.S. Camarda, Y. Cui, R.B. James, Optimization of selenium in CdZnTeSe quaternary compound for radiation detector applications, *Appl. Phys. Lett.* **118**, 152101 (2021). https://doi.org/10.1063/5.0048875
7. U.N. Roy, C.T. Trinh, H. Htoon, A.C. Jones, R. Cortes-Robles, A.A. Egarievwe, G.S. Camarda, S.U. Egarievwe, M. Drabo, R.B. James, Spatial variation of the low-temperature micro-photoluminescence of THM-grown CdZnTeSe, *Materials Today Comm.* **42**, 111486 (2025). https://doi.org/10.1016/j.mtcomm.2024.111486
8. C. Szeles, M.C. Driver, Growth and properties of semi-insulating CdZnTe for radiation detector applications, SPIE Conf. on Hard X-Ray and Gamma-Ray Detector Physics and Applications, San Diego, California, July 1998, Proc. SPIE **3446**, 1 (1998). http://dx.doi.org/10.1117/12.312878
9. F. Yang, W. Jie, M. Wang, X. Sun, N. Jia, L. Yin, B. Zhou, T. Wang, Growth of Single-Crystal Cd0.9Zn0.1Te Ingots Using Pressure Controlled Bridgman Method, *Crystals* **10**(4), 261 (2020). https://doi.org/10.3390/cryst10040261
10. A.M. Martinez, P. Giudici, A.B. Trigubo, R. D'Elia, E. Heredia, R. Ramelli, R. Gonzalez, F. Aza, U. Gilabert, Crystalline Quality, Composition Homogeneity, Tellurium Precipitates/Inclusions Concentration, Optical Transmission, and Energy Band Gap of Bridgman Grown Single-

Crystalline $Cd_{1-x}Zn_xTe$ ($0 \le x \le 0.1$), *Materials* **14**(15), 4207 (2021). https://doi.org/10.3390/ma14154207

11. J.J. McCoy, S. Kakkireni, Z.H. Gilvey, S. K. Swain, A.E. Bolotnikov, K.G. Lynn, Overcoming Mobility Lifetime Product Limitations in Vertical Bridgman Production of Cadmium Zinc Telluride Detectors, J. of Electronic Materials **48**, 4226-4234 (2019). https://doi.org/10.1007/s11664-019-07196-5
12. M. Unal, O.B. Balbasi, S.H. Sedani, M.C. Karaman, G. Celik, D. Bender, A.M. Genc, M. Parlak, R. Turan, Production of detector grade CdZnTe crystal with VGF furnace by analyzing segregation of Zn and In, *J. of Crystal Growth* **615**, 127236 (2023). https://doi.org/10.1016/j.jcrysgro.2023.127236
13. H. Chen, S.A. Awadalla, K. Iniewski, P.H. Lu, F. Harris, J. Mackenzie, T. Hasanen, W. Chen, R. Redden, G. Bindley, I. Kuvvetli, C. Budtz-Jorgensen, P. Luke, M. Amman, J.S. Lee, A.E. Bolotnikov, G.S. Camarda, Y. Cui, A. Hossain, R.B. James; Characterization of large cadmium zinc telluride crystals grown by traveling heater method, *J. Appl. Phys.* **103**(1), 014903 (2008). https://doi.org/10.1063/1.2828170
14. B. Hong, S. Zhang, L. Zheng, H. Zhang, C. Wang, B. Zhao, Studies on thermal and interface optimization for CdZnTe crystals by unseeded Traveling Heater Method, *J. of Crystal Growth* **546**, 125776 (2020). https://doi.org/10.1016/j.jcrysgro.2020.125776
15. J.W. Kleppinger, S.K. Chaudhuri, U.N. Roy, R.B. James, K.C. Mandal, Growth of Cd0.9Zn0.1Te1-ySey single crystals for room temperature gamma-ray detection, *IEEE Trans. on Nucl. Sci.* **68**(9), 2429-2434 (2021). http://dx.doi.org/10.1109/TNS.2021.3077505
16. L. Martinez-Herraiz, A.F. Brana, J.L. Plaza, Vertical Gradient Freeze growth of two inches Cd1-xZnxTe1-ySey ingots with different Se content, *J. of Crystal Growth* **573**, 126291 (2021). https://doi.org/10.1016/j.jcrysgro.2021.126291
17. K. Kim, J. Franc, A.E. Bolotnikov, R.B. James, Photoluminescence of CdTe and CdZnTe compounds doped with 2% selenium, *J. of Crystal Growth* **626**, 127478 (2024). https://doi.org/10.1016/j.jcrysgro.2023.127478
18. Q. Zheng, J. Crocco, H. Bensalah, P. Wellmann, A. Osvet, U. Kunecke, F. Dierre, O. Vela, J.M. Perez, E. Dieguez, Influence of the starting materials used in the crystal growth process of CZT for gamma ray radiation applications, *J. of Crystal Growth* **381,** 15-21 (2013). http://dx.doi.org/10.1016/j.jcrysgro.2013.06.033
19. U.N. Roy, G.S. Camarda, Y. Cui, R.B. James, Advances in CdZnTeSe for radiation detector applications, *Radiation*, **1**(2), 123-130 (2021). https://doi.org/10.3390/radiation1020011
20. P. Atkins, J. de Paula, J. Keeler, Physical Chemistry, 12th edition, Oxford University Press, New York, 2023.
21. B. Park, Y. Kim, J. Seo, J. Byun, V. Dedic, J. Franc, A.E. Bolotnikov, R.B. James, K. Kim, Bandgap engineering of of Cd1-xZnxTe1-ySee ($0 < x < 0.27$, $0 < y < 0.026$), *Nucl. Instrum. Methods in Phys. Research Sec. A*, **1036**, 166836 (2022). https://doi.org/10.1016/j.nima.2022.166836
22. E. Scheil, Über die Eutektische Kristallization, *Zeitschrift für Metallkunde* **34**, 70-76 (1942). https://doi.org/10.1515/ijmr-1957-480904
23. A. Yakimov, D.J. Smith, J. Choi, S.L. Araujo, Growth and characterization of detector-grade CdZnTeSe by horizontal Bridgman technique, Proc. SPIE **11114**, Hard X-ray, Gamma-Ray, and Neutron Detector Physics XXI, 111141N (2019). https://doi.org/10.1117/12.2528542
24. L. Martinez-Herraiz, A.F. Brana, J.L. Plaza, Vertical Gradient Freeze Growth of two inches $Cd_{1-x}Zn_xTe_{1-y}Se_y$ ingots with different Se content, Journal of Crystal Growth **573**, 126291 (2021). https://doi.org/10.1016/j.jcrysgro.2021.126291